DNA Damage Induced Hyperphosphorylation of Replication Protein A. 2. Characterization of DNA Binding Activity, Protein Interactions, and Activity in DNA Replication and Repair†

Steve M. Patrick,‡,§ Greg G. Oakley,#,§ Kathleen Dixon,⊥ and John J. Turchi*,‡

Department of Biochemistry and Molecular Biology, Wright State University School of Medicine, Dayton, Ohio 45435, Department of Environmental Health, University of Cincinnati College of Medicine, Cincinnati, Ohio 45267, and Department of Molecular and Cellular Biology, University of Arizona, Tucson, Arizona 85721-0106

Received September 9, 2004; Revised Manuscript Received April 13, 2005

ABSTRACT: Replication protein A (RPA) is a heterotrimeric protein consisting of 70-, 34-, and 14- kDa subunits that is required for many DNA metabolic processes including DNA replication and DNA repair. Using a purified hyperphosphorylated form of RPA protein prepared in vitro, we have addressed the effects of hyperphosphorylation on steady-state and pre-steady-state DNA binding activity, the ability to support DNA repair and replication reactions, and the effect on the interaction with partner proteins. Equilibrium DNA binding activity measured by fluorescence polarization reveals no difference in ssDNA binding to pyrimidine-rich DNA sequences. However, RPA hyperphosphorylation results in a decreased affinity for purine-rich ssDNA and duplex DNA substrates. Pre-steady-state kinetic analysis is consistent with the equilibrium DNA binding and demonstrates a contribution from both the k_{on} and k_{off} to achieve these differences. The hyperphosphorylated form of RPA retains damage-specific DNA binding, and, importantly, the affinity of hyperphosphorylated RPA for damaged duplex DNA is 3-fold greater than the affinity of unmodified RPA for undamaged duplex DNA. The ability of hyperphosphorylated RPA to support DNA repair showed minor differences in the ability to support nucleotide excision repair (NER). Interestingly, under reaction conditions in which RPA is maintained in a hyperphosphorylated form, we also observed inhibition of in vitro DNA replication. Analyses of protein−protein interactions bear out the effects of hyperphosphorylated RPA on DNA metabolic pathways. Specifically, phosphorylation of RPA disrupts the interaction with DNA polymerase α but has no significant effect on the interaction with XPA. These results demonstrate that the effects of DNA damage induced hyperphosphorylation of RPA on DNA replication and DNA repair are mediated through alterations in DNA binding activity and protein−protein interactions.

Replication protein A (RPA)[1] has fundamental roles in numerous DNA metabolic pathways, which include DNA replication, DNA repair, and DNA recombination. RPA is the major single-stranded DNA (ssDNA) binding protein in the eukaryotic cell. This DNA binding activity along with the specific interaction with numerous proteins involved in DNA metabolism are required to maintain the individual DNA metabolic pathways that contribute to genome propagation and stability (*1*). With multiple roles in DNA metabolism, it is tempting to speculate that altering RPA activity could influence regulation of these specific pathways. In fact, the p34 subunit of RPA becomes phosphorylated in a cell cycle and DNA damage-specific manner, but conflicting data exist on the effects of RPA phosphorylation on the activities of RPA and its role in DNA metabolic pathways (*2*).

RPA interacts with several proteins involved in nucleic acid metabolism, including DNA polymerase α, simian virus 40 (SV40) large T antigen, XPA, XPG, XPF-ERCC1, DDB, proteins in the Rad52 epistasis group, and the Blooms and Werners helicases (*3*−*10*). RPA has also been shown to interact with proteins involved in cell cycle control and the DNA damage response pathways including p53, cdc2, DNA-PK, and ATM (*11*−*14*). The DNA damage-dependent phosphorylation of RPA was found to disrupt its interaction with p53 (*15*). An in vitro phosphorylated form of RPA was shown to have no effect on the interaction with XPA (*16*). More recently, we have shown that a highly purified mitotic specific phosphorylated form of RPA displayed altered interactions with ATM, DNA-PK, and DNA pol α, while no alteration was observed with XPA (*11*).

The effect of RPA phosphorylation on RPA DNA binding activity has recently been the focus of two reports. We have

† This work was supported by Public Health Service Grant CA82741 to J.J.T. from the National Cancer Institute and Public Health Service Grants NS34782 and ES06096 and a research grant from the A-T Children's Project to K.D.

* To whom correspondence should be addressed. Tel: (937)-775-3595; fax: (937)-775-3730; e-mail: john.turchi@wright.edu.

‡ Wright State University School of Medicine.

University of Cincinnati College of Medicine.

⊥ University of Arizona.

§ These authors contributed equally to this work.

[1] Abbreviations: RPA, replication protein A; XPA, xeroderma pigmentosum group A protein; ssDNA, single-stranded DNA; dsDNA, double-stranded DNA; CIP, calf intestinal phosphatase; PAGE, polyacrylamide gel electrophoresis; NER, nucleotide excision repair.

10.1021/bi048057b CCC: $30.25
Published on Web 05/21/2005

demonstrated that the mitotic phosphorylated form of RPA displayed a reduced affinity for duplex DNA that was a result of an alteration in the denaturation activity of RPA (*11*). Interestingly, phosphorylation of RPA had no effect on high-affinity ssDNA binding activity. These results were recently confirmed using a mutant RPA in which eight serine/threonine residues of the N-terminus of the p34 subunit of RPA were changed to aspartic acids and a decrease in DNA denaturation activity was also observed (*17*).

It has been demonstrated that RPA phosphorylation has no effect on nucleotide excision repair (NER) in both a highly purified reconstituted system as well as in crude extract analysis in vitro (*18*). The addition of okadaic acid (a phosphatase inhibitor) to cell extracts inhibited NER and resulted in RPA hyperphosphorylation. The phosphorylation status of RPA, however, was suggested to play no role in NER due to the inability of unphosphorylated RPA to restore incision activity in the okadaic acid-inhibited cell extract (*19*). This supports the hypothesis that RPA phosphorylation has no effect on DNA repair, enabling cells to maintain active DNA repair complexes following DNA damage. In addition, a cdk/cyclin A, DNA-PK-dependent in vitro phosphorylated form of RPA was found to act equally well in an in vitro NER assay (*18*).

While the results with in vitro NER are very consistent, there appears to be some controversy as to whether RPA phosphorylation affects DNA replication. UV-induced DNA damage results in hyperphosphorylation of RPA, and extracts prepared from these cells displayed a reduction in the ability to support DNA replication as measured in the SV40 in vitro replication system (*20*). The addition of purified unphosphorylated RPA restored replication activity, suggesting that the inhibition of replication was a result of the phosphorylation of RPA. Extracts prepared from cells treated with the DNA intercalating agent adozelesin as well as other DNA damaging agents also revealed the same result, a decrease in replication activity that could be overcome by the addition of purified unphosphorylated RPA (*21*, *22*). Together these results provide considerable evidence that DNA damage-dependent phosphorylation of RPA can affect DNA replication. However, reproduction of these results using purified phosphorylated RPA in an in vitro SV40 based assay has yet to be demonstrated. A cdk-cyclinA and DNA-PK phosphorylated form of RPA was fully capable of supporting DNA replication in a monopolymerase system, which uses a subset of proteins required for DNA replication (*18*). In addition, the phosphorylated RPA was capable of complementing crude cellular fractions to restore DNA replication. These results suggest that the phosphorylation of RPA has no effect on replication machinery. The discrepancies between these studies may lie in the levels of RPA phosphorylation and the sites of phosphorylation, which we have mapped to both the p34 and p70 subunits (accompanying manuscript in this issue, *23*). In this study, we have prepared an in vitro phosphorylated form of RPA that exhibits a reduced ability to support DNA replication. We have also investigated the role of RPA hyperphosphorylation on ssDNA binding, double-stranded DNA (dsDNA) binding, and protein−protein interactions to determine the mechanism by which hyperphosphorylated RPA exerts its effect on DNA metabolism. The data along with the identification of specific sites of phosphorylation provide a comprehensive analysis of a hyperphosphorylated form of RPA and its activities in DNA metabolic pathways.

MATERIALS AND METHODS

Materials. DNA oligonucleotides were purchased from Integrated DNA Technologies (IDT), Inc. (Coralville, IA). Mung bean nuclease, T4 polynucleotide kinase, and T4 DNA ligase were from New England Biolabs (Beverly, MA). Radiolabeled nucleotides were purchased from PerkinElmer Life Sciences (Boston, MA), and the unlabeled nucleotides were from Amersham Biosciences. Anti-p34 RPA monoclonal antibody (RPA/p32 Ab-1) and the anti-p70 RPA monoclonal antibody (RPA/p70 Ab-2) were purchased from NeoMarkers (Fremont, CA). Large T-Ag was purchased from Chimerx (Madison, WI). Protein G-Agarose was from Invitrogen and the cisplatin was from Sigma. All other reagents, chemicals, and enzymes were from standard suppliers.

DNA Substrate Preparation and Platination. All DNA substrates were purified by preparative DNA sequencing gels prior to use. DNA substrates for the electrophoretic mobility shift assays (EMSAs) were purified and labeled as previously described (*24*). Briefly, the DNA substrates were labeled using T4 polynucleotide kinase and [γ-^{32}P]ATP. The duplex DNA substrates used in the stopped-flow experiments were purified as previously described (*24*−*26*). The DNA substrates used for anisotropy were identical to those used previously except for a 5′-fluorescein modification, and the duplex DNA's were purified as described (*27*). Briefly, the fluorescein-labeled DNA was annealed to the complementary DNA sequence and gel purified on 15% native polyacrylamide gels to separate the ssDNA from duplex DNA. All the duplex DNA substrates used had less than 5% ssDNA contamination. The oligonucleotides treated with cisplatin were incubated in 1 mM $NaHPO_4$ (pH 7.5) and 3 mM NaCl for 16−20 h at 37 °C in the dark. The DNA was treated at a 4:1 molar ratio of cisplatin to d(GpG) or d(GpXpG) sites. The unreacted cisplatin was removed by G-50 spin column chromatography or ethanol precipitation followed by washing with 70% ethanol (*25*). Prior to gel purification, the DNAs were treated with Hae III or Aci I, which cleaves the undamaged DNA and ensures that all DNA substrates are platinated. The 120 bp DNA substrate used in the in vitro incision assay was purified as previously described (*28*).

Protein Purification. Recombinant human RPA (rhRPA) was purified as previously described using the expression vector provided by Wold (*24*). Hyperphosphorylated RPA was purified by using a modified protocol from previously published procedures (*18*, *19*, *24*). *Escherichia coli* extracts containing RPA were prepared and fractionated on a ssDNA cellulose column in buffer containing 25 mM Tris-HCl (pH 7.5), 1 mM EDTA, 1 mM DTT, 0.01% Triton X-100, 10% glycerol, and 0.5 M NaCl. Bound RPA protein was eluted with the same buffer containing 2 M NaCl, and the resulting RPA fraction was approximately 80% pure. The RPA was dialyzed in DNA repair buffer (45 mM HEPES pH 7.8, 70 mM KCl, 7.4 mM $MgCl_2$, 0.9 mM DTT, 0.4 mM EDTA, and 3.4% glycerol) and mixed with HeLa extracts (220 mg) containing the same buffer. Prior to the incubation, 2 mM ATP, 22 mM phosphocreatine, 50 μg/mL creatine phosphokinase, and 5 μg/mL calf thymus DNA were added to the

reaction. The mixture was also supplemented to 4 μM okadaic acid, 5 nM microcystin LR, 5 μM cantharidin, and 25 μM *p*-bromotetramisole oxalate to inhibit phosphatase activity within the cell extracts. This reaction allowed endogenous kinases within the HeLa extract to phosphorylate the RPA. Following incubation for 3 h at 30 °C, the hyperphosphorylated RPA was purified in an identical manner to recombinant RPA. All buffers were supplemented with 5 nM microcystin LR, 5 μM cantharidin, and 25 μM *p*-bromotetramisole oxalate. RPA protein was separated on 13% SDS−PAGE and stained with Coomassie or transferred to immobilon P polyvinyl-divinyl fluoride (PVDF) transfer membranes (Millipore Corp., Bedford, MA) and used for Western blot analysis as previously described (*11*). Active protein for both the rhRPA and the hyperphosphorylated RPA were determined by DNA binding to dT30 ssDNA.

XPA was purified using metal chelate affinity chromatograph following expression in Sf-21 insect cells as previously described (*28*). DNA pol α was purified from calf thymus by immunoaffinity chromatography (*29*).

Electrophoretic Mobility Shift Assays (EMSAs). DNA binding assays were performed in the presence of 20 mM HEPES (pH 7.8), 2 mM dithiothreitol, 0.001% Nonidet P-40, and 50 mM NaCl. The duplex DNA binding assays contained 50 fmol of labeled DNA and the indicated amount of RPA. The RPA or hyperphosphorylated RPA was incubated with DNA for 15 min at room temperature followed by the addition of gel loading buffer. The products were separated on 4% native polyacrylamide gels as previously described (*25*). RPA-p34 antibody was added for 10 min after initial incubation of RPA with the DNA to supershift the RPA−DNA complex.

Anisotropy. Anisotropy values (*r*) were calculated using eq 1 from fluorescence intensities measured with emission and excitation polarizers set either parallel ($I_{||}$) or perpendicular ($I_{\perp}$)to each other. The fluorescence for vertical and

$$r = \frac{I_{||} - I_{\perp}}{I_{||} + 2I_{\perp}} \quad (1)$$

horizontal emission was corrected using the G factor calculated using the fluorescein DNA substrate in the appropriate buffer as the depolarizing sample. All experiments were performed using a Cary Eclipse Fluorescence spectrophotometer (Varian). Fluorescence was monitored at 515 nm following excitation at 495 nm. The bandwidths for both excitation and emission monochromators were set at 10 nm. Reactions were prepared and allowed to equilibrate at room temperature. Following equilibration, five data points were taken with 5 s intervals for each titration point. Anisotropy measurements were performed in buffer containing 20 mM HEPES (pH 7.8), 0.001% NP-40, 2 mM DTT, 50 mM NaCl, and 2 mM $MgCl_2$, except for the dT_{30} ssDNA reactions, which were performed in the presence of 1 M NaCl. Duplex and ssDNA were included in reactions at 10 and 0.5 nM, respectively. The fluorescence reactions were performed in a 400 μL cuvette for the ssDNA with a final volume of 500 μL and a 40 μL cuvette for the duplex DNA substrates with a final volume of 100 μL. The RPA concentration in each reaction is indicated in the figure legends.

Stopped-Flow Kinetic Analysis of RPAs DNA Binding Activity. The stopped-flow kinetic traces for DNA binding were obtained using a SX.18MV reaction analyzer (Applied Photophysics) as previously described (*26*, *30*). The DNA substrates used for the stopped-flow experiments were unlabeled but were prepared identically as those used in the EMSAs. The purine-rich 30-mer ssDNA substrate was used previously (*26*). The DNA binding buffer was identical to that used in the EMSA with the exception that 2 mM $MgCl_2$ was added to the reactions for the ssDNA. The $MgCl_2$ was not added in the duplex DNA reactions because the $MgCl_2$ stabilizes the duplex DNA structure creating more stringent conditions. This results in reduced k_{on} values and nearly undetectable DNA binding for the hyperphosphorylated RPA (data not shown). The observed rates, k_{obs}, obtained from the kinetic traces were plotted versus DNA concentration, resulting in a linear relationship with the slope equal to the association rate, k_{on}. The traces used to generate the k_{obs} data represent the average of 10−12 individual shots. The individual points on the graph for determining the k_{on} are the average of at least three experiments with the error bars representing the standard deviation.

In Vitro Nucleotide Excision Repair Assay. An in vitro DNA incision assay using cell-free HeLa extracts was employed similar to that previously described (*28*). The reaction mixtures (25 μL) contained 10 fmol of internally labeled 120 bp DNA containing a single cisplatin d(GpXpG) adduct. Reactions were initiated with 100 μg of HeLa extract in buffer containing 45 mM HEPES (pH 7.8), 70 mM KCl, 7.4 mM $MgCl_2$, 0.9 mM DTT, 0.4 mM EDTA, 3.4% glycerol, 5 μg of BSA, 2 mM ATP, 20 μM each of dATP, dCTP, dGTP, and dTTP, 22 mM phosphocreatine, and 1.25 μg of creatine phosphokinase. The reactions were incubated for 30 min at 30 °C. Immunodepletion of RPA from the extracts was performed using a monoclonal antibody directed against the p70 subunit (RPA/p70 Ab-2) and protein G agarose. Complementation of the immunodepleted extracts was performed with the addition of 300 ng of either RPA or hyperphosphorylated RPA as indicated in the figure legend. Okadaic acid was added to 0.1 μM in the indicated reactions to inhibit dephosphorylation of hyperphosphorylated RPA during the DNA repair assay. After the 30 min incubation, the reactions were stopped by the addition of EDTA to a concentration of 10 mM. A 5 μL aliquot of the reaction was used for the Western blot analysis. Proteinase K was added to the repair reactions and subsequently incubated for 30 min at 37 °C. The DNA was ethanol precipitated and resuspended in gel loading buffer, and products were separated on 8% polyacrylamide−7 M urea sequencing gels and visualized by autoradiography.

In Vitro DNA Replication Assay and Preparation of Cell Extracts. Hypotonic cell extracts were prepared (*31*), and DNA replication assays were carried out as previously described (*32*). Briefly, replication reactions (30 μL) contained 25 ng of the SV40-based plasmid, pZ189, (*33*) as the DNA template; 80 μg of HeLa extract protein; 30 mM Hepes (pH 7.5); 100 mM each of dATP, dGTP, and dTTP; 50 mM dCTP; 10 mCi [α-^{32}P]dCTP; 200 mM each of GTP, UTP, CTP; 4 mM ATP; 40 mM creatine phosphate; 10 μg of creatine phosphokinase; and 1 μg of SV40 large T antigen. Immunodepletion of RPA from the HeLa extracts was carried out essentially as described above. Where indicated, either

RPA (150 ng) or hyperphosphorylated RPA (150 ng) was added to the immunodepleted extracts as indicated in the figure legend. Replication reactions were incubated at 37 °C for 2 h and terminated by addition of EDTA to 15 mM and proteinase K to 1 μg/mL, followed by incubation at 37 °C for 30 min. DNA was purified from replication reactions by extraction with phenol and with chloroform. Unincorporated radionucleotides were removed by spin dialysis against TE (pH 7.5), using a Centricon 30 centrifugal filter device (Millipore Corp., Bedford MA). To remove unreplicated DNA, purified plasmid DNA was treated with DpnI. DpnI reactions consisted of DpnI (0.15 U) in 6 mM Tris-HCl (pH 7.5), 150 mM NaCl, 6 mM $MgCl_2$, 7 mM β-mercaptoethanol, and 100 μg/mL bovine serum albumin incubated for 1 h at 37 °C. DNA was purified and analyzed by electrophoresis on a 1% agarose gel run in 1 X Tris-acetate-EDTA (TAE) buffer containing 5 μg/mL ethidium bromide, followed by autoradiography and quantification by phosphorImager analysis.

Immunoprecipitation and Immunoblot Analysis. For co-immunoprecipitation assays, 100 ng of RPA or hyperphosphorylated RPA was incubated with either 500 ng of purified XPA or DNA pol α in phosphate-buffered saline containing 0.05% NP-40 for 30 min with end-over-end mixing at 4 °C. Following the addition of 0.5−3.0 μg of anti-XPA or DNA pol α antibody, the immunoprecipitates were incubated overnight at 4 °C. After the addition of 30 μL of protein G-agarose (Gibco-BRL) for 2 h, the immunoprecipitates were separated from the supernatant by centrifugation at 5000*g* for 5 min. The immunoprecipitates were washed three times with 0.01% NP-40-PBS, resuspended in 1× Laemmli gel loading buffer. The immunoprecipitates and aliquots from the supernatants were fractionated on a 13% SDS−polyacrylamide gel and subjected to immunoblot analysis as previously described (*11*).

ELISA Assays to Measure Protein−Protein Interactions. ELISA assays were performed as described previously (*28*). Briefly, flat-bottomed 96-well ELISA plates were coated with 0.86 pmol of RPA or hyperphosphorylated RPA protein and incubated at 37 °C for 3 h. Unbound protein was removed, and wells were rinsed. The wells were blocked by the addition of 200 μL of blocking buffer (5% NFDM in PBS) and incubated overnight at 4 °C. Blocking buffer was removed from the wells, plates were rinsed, and the relevant secondary protein was added at a 0.5×, 1×, or 2× molar ratio and incubated at room temperature for 1 h. Plates were then rinsed, and bound secondary protein was detected with the relevant primary and HRP-conjugated secondary antibodies. HRP activity was monitored following the addition of 200 μL of TMB-ELISA reagent (Gibco BRL, Life Technologies, Gaithersburg, MD) to each well. The change in absorbance at 650 nm was monitored at 30-s intervals for 15 min and analyzed using SoftMax Pro software (Molecular Devices Corp., Sunnyvale, CA). Relative binding activity is based on HRP activity that is determined as the change in absorbance at 650 nm/min. The reactions displayed linear kinetics for the duration of the assay (data not shown).

RESULTS

RPA Hyperphosphorylation Differentially Alters ssDNA Binding. ssDNA binding is a fundamental role for RPA in DNA metabolic pathways. While it is becoming clear that phosphorylation of RPA can alter its ability to bind specific DNA substrates, many of the assays used to assess this binding rely on electrophoretic mobility shift analyses (EMSAs) where an accurate kinetic analysis and the separate contributions of the k_{on} and k_{off} can be obscured during the electrophoretic separation. We have purified a hyperphosphorylated form of RPA and characterized the sites and extent of phosphorylation (accompanying manuscript in this issue, *23*) Our initial results using EMSA of this form of RPA revealed that phosphorylation had no affect on RPA binding pyrimidine-rich ssDNA (data not shown). To address whether hyperphosphorylation affects RPA ssDNA binding affinity under true solution-based equilibrium DNA binding conditions, we have employed a fluorescence anisotropy assay to measure the formation of protein−DNA complexes in solution. Fluorescein 5′-labeled DNA substrates were used as the fluorescent probes in the RPA titration experiments. In solution, free fluorescein has a rapid rotational motion with respect to fluorescence lifetime. Following excitation with a vertical polarizer, the emitted fluorescence is entirely depolarized. The coupling of fluorescein to DNA results in a slower rotational motion which results in an increased anisotropy (*r* value). The addition of a DNA binding protein, RPA, to the fluorescein-labeled DNA further increases the anisotropy. The change in anisotropy with increasing RPA is a direct reflection of RPA−DNA complex formation. Analysis of rhRPA and hyperphosphorylated RPA binding to a dT_{30} substrate was performed, and in the reactions containing 50 mM NaCl stoichiometric binding was observed, consistent with an extremely slow k_{off} under these conditions (data not shown). To achieve nonstoichiometric equilibrium binding conditions, NaCl was added to the reactions to a final concentration of 1 M. The results presented in Figure 1A demonstrate that RPA binding to a dT_{30} DNA substrate is well described by a single-step binding reaction and that RPA binding affinity is unaffected by hyperphosphorylation. Fitting the data obtained from RPA titration experiments to the equation for a rectangular hyperbole yielded equilibrium dissociation constants of 7.6 $\pm$ 0.8 and 6.2 $\pm$ 0.5 nM for rhRPA and hyperphosphorylated RPA, respectively. These data demonstrate that under true equilibrium conditions, hyperphosphorylation of RPA does not alter its affinity for pyrimidine-rich ssDNA substrates.

We have previously used a highly sensitive pre-steady-state kinetic analysis to measure rhRPA binding constants to various DNA substrates (*26*). The stopped-flow methodology utilizes the intrinsic fluorescence of RPA and monitors the quenching of fluorescence upon RPA binding to DNA. To confirm the steady-state DNA binding data and establish an association rate, k_{on}, for hyperphosphorylated RPA binding ssDNA, we performed the stopped-flow analysis measuring the interaction with the dT_{30} ssDNA. A DNA concentration- and time-dependent quenching was observed with the hyperphosphorylated RPA, and the traces were fit to a single-exponential decay curve, consistent with that published with rhRPA. The observed rate, k_{obs}, was plotted versus DNA concentration, yielding a linear fit with the slope indicating the k_{on} (Figure 1B). The k_{on} for hyperphosphorylated RPA binding the dT_{30} ssDNA was determined to be 1.96 $\pm$ 0.19 nM^{-1} s^{-1}, while the k_{on} determined for rhRPA binding dT_{30} ssDNA was 2.14 $\pm$ 0.08 nM^{-1} s^{-1} (*26*). These data support

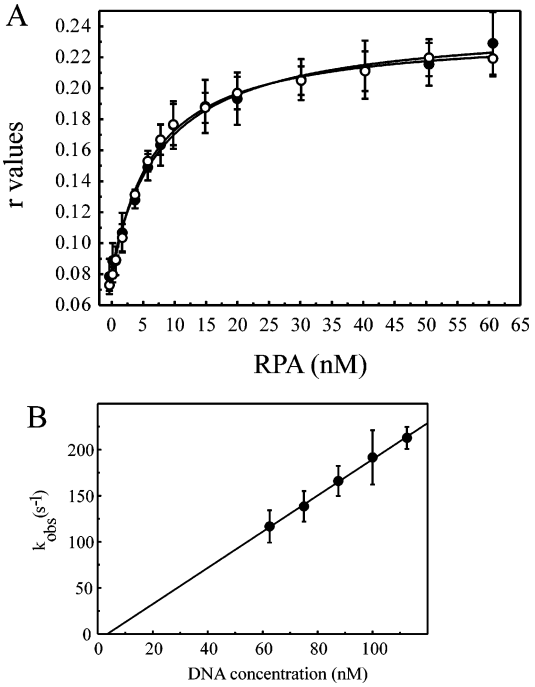

FIGURE 1: Anisotropy and stopped-flow kinetic analysis of hyperphosphorylated RPA binding pyrimidine ssDNA. (A) Fluorescence polarization analysis of RPA (filled circles) and hyperphosphorylated RPA (open circles) binding to dT_{30} DNA substrates in reactions supplemented with 1 M NaCl. (B) Kinetic traces were performed at a constant RPA concentration (6.25 nM) and increasing concentrations of DNA (62.5, 75, 87.5, 100, and 112.5 nM). The traces were fit to a single-exponential decay. The observed rate constants (k_{obs}) were plotted versus DNA concentration and fit to a straight line. The slope of the line provides the bimolecular rate constant, k_{on}, for hyperphosphorylated RPA binding the dT_{30} ssDNA. Each point on the graph represents the average of at least three individual experiments, and the error bars represent the standard deviation.

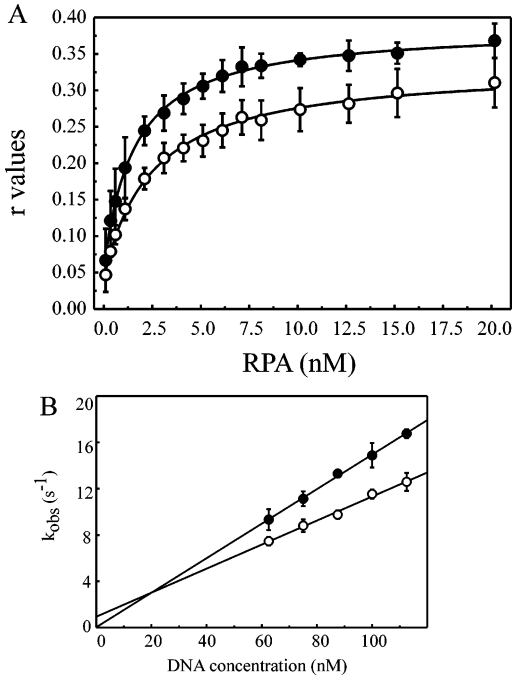

FIGURE 2: Anisotropy and stopped-flow analysis of RPA binding purine ssDNA. (A) Fluorescence polarization analysis of RPA (filled circles) and hyperphosphorylated RPA (open circles) binding to a purine-rich 30 base DNA substrate. (B) Stopped-flow kinetic analysis of RPA binding purine ssDNA. The plot of k_{obs} versus DNA concentration for rhRPA (filled circles) and hyperphosphorylated RPA (open circles) binding to a 30 bp purine-rich DNA are presented. The points on the graph are the average of three to four separate experiments, and the error bars represent the standard deviation.

the anisotropy results and demonstrate that there is no difference in RPA binding to a pyrimidine-rich ssDNA substrate.

Considering the extremely high affinity of RPA for dT30, small differences in the interaction may be difficult to detect in this analysis. Therefore, we have determined the effect of RPA phosphorylation on its affinity for a series of DNA substrates. Considering that RPA has a 30−50-fold higher affinity for pyrimidine-rich DNA compared with purine-rich DNA, we first assessed RPA binding to a purine-rich 30-mer ssDNA substrate. RPA has a considerably lower affinity for purine-rich DNA sequences as a result of a reduced rate of association and a slight increased rate of dissociation (*26*). Considering the ability of RPA to bind a variety of different DNA substrates, the possibility existed that hyperphosphorylation of RPA could differentially alter its affinity for the different DNA structures. DNA binding titrations using a purine-rich ssDNA were therefore performed, and the results are presented in Figure 2A. Values for equilibrium dissociation constants obtained in the titration experiments yielded K_d values of 1.66 ± 0.1 and 2.55 ± 0.2 nM for rhRPA and hyperphosphorylated RPA, respectively. These K_d values are lower than those obtained for the pyrimidine-rich DNA as a result of performing the reaction in 50 mM NaCl instead of 1 M NaCl. Despite the lower K_d values for this substrate under these conditions, a significant decrease in the affinity of the hyperphosphorylated RPA for the purine-rich ssDNA was observed compared to the unphosphorylated RPA. The observation that the maximum *r*-values obtained is different between the rhRPA and hyperphosphorylated RPA is likely a result of the protein−DNA complexes being slightly different in size or shape such that the maximum rotation is different. This difference, however, does not influence the K_d values calculated from each curve.

Stopped-flow kinetic analysis was performed with rhRPA and hyperphosphorylated RPA in a manner identical to the experiments performed with the dT_{30} ssDNA. The k_{obs} values were again plotted versus DNA concentration with the slope of the line being equal to the k_{on} (Figure 2B). The results demonstrate that the hyperphosphorylated RPA has a reduced k_{on} (0.105 ± 0.006 nM^{-1} s^{-1}) compared with the rhRPA (0.149 ± 0.008 nM^{-1} s^{-1}). These data suggest that RPA hyperphosphorylation can alter ssDNA binding to purine-rich substrates. The k_{on} of RPA for pyrimidine-rich DNA is at or near the diffusion limit and is 10−15 times faster than the k_{on} for purine-rich DNA; this may explain why phosphorylation-dependent differences in DNA binding were seen with the purine-rich ssDNA but not with the pyrimidine-rich ssDNA.

Hyperphosphorylation of RPA Results in a Reduced Affinity for Duplex DNA. The affinity of RPA for duplex DNA substrates is considerably lower than that observed for ssDNA. We have previously shown that RPA preferentially binds to duplex cisplatin-damaged DNA and that this DNA binding correlates with the ability of RPA to denature these DNA substrates (*24*). The affinity of RPA for duplex DNA correlates with the degree of thermal instability of the duplex

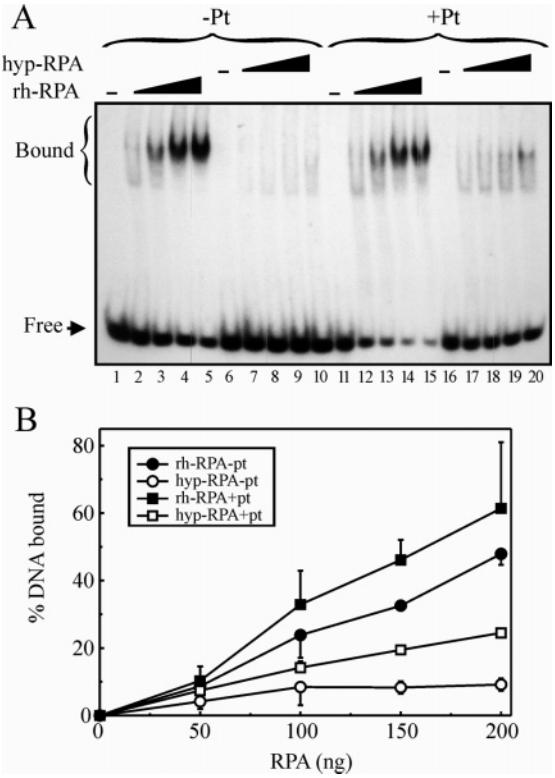

FIGURE 3: Hyperphosphorylated RPA binding duplex undamaged and cisplatin-damaged 30-mer DNA. (A) EMSAs were performed using the following indicated amounts of rhRPA (lanes 1−5 and 11−15) or hyperphosphorylated RPA (lanes 6−10 and 16−20) and 50 fmol of either 30 bp undamaged (lanes 1−10) or 1,2d(GpG) cisplatin-containing DNA (lanes 11−20). The products were separated on a 4% native polyacrylamide gel and visualized by autoradiography. Lanes 1, 6, 11, and 16 without added RPA; lanes 2, 7, 12, and 17, 50 ng (425 fmol) RPA; lanes 3, 8, 13, and 18, 100 ng (850 fmol); lanes 4, 9, 14, and 19, 150 ng (1.275 pmol); lanes 5, 10, 15, and 20, 200 ng (1.7 pmol). (B) Quantification of increasing concentrations of rhRPA (filled symbols) and hyperphosphorylated RPA (open symbols) binding undamaged (circles) and 1,2d(GpG) cisplatin-damaged DNA (squares). The results are the average of two individual experiments, and the error bars represent the range of values.

DNA. Cisplatin adducts on DNA result in a distortion of the duplex DNA structure and reduced thermal stability with the cisplatin 1,2d(GpG) adduct being moderately distorting and the 1,3d(GpXpG) adduct being highly distorting. To determine if RPA phosphorylation affects duplex DNA binding, EMSAs were conducted using a duplex 30 bp DNA in the absence or presence of a cisplatin 1,2d(GpG) DNA adduct. With increasing rhRPA, an increase in duplex DNA binding is observed for both the undamaged and cisplatin-damaged DNA (Figure 3A, lanes 1−5 and lanes 11−15, respectively), consistent with our previously published results. To detect binding of the hyperphosphorylated form of RPA to the duplex DNA substrates, $MgCl_2$ was omitted from the reactions; this results in greater binding to the duplex DNA at the expense of damage specificity (*25*). The hyperphosphorylated form of RPA binds minimally to the undamaged duplex DNA (Figure 3A, lanes 6−10), while somewhat increased binding is observed in the presence of the cisplatin 1,2d(GpG) DNA adduct (Figure 3A, lanes 16−20). Quantification of the results reveals preferential DNA binding of both rhRPA and the hyperphosphorylated RPA to the cisplatin-damaged DNA compared with the undamaged

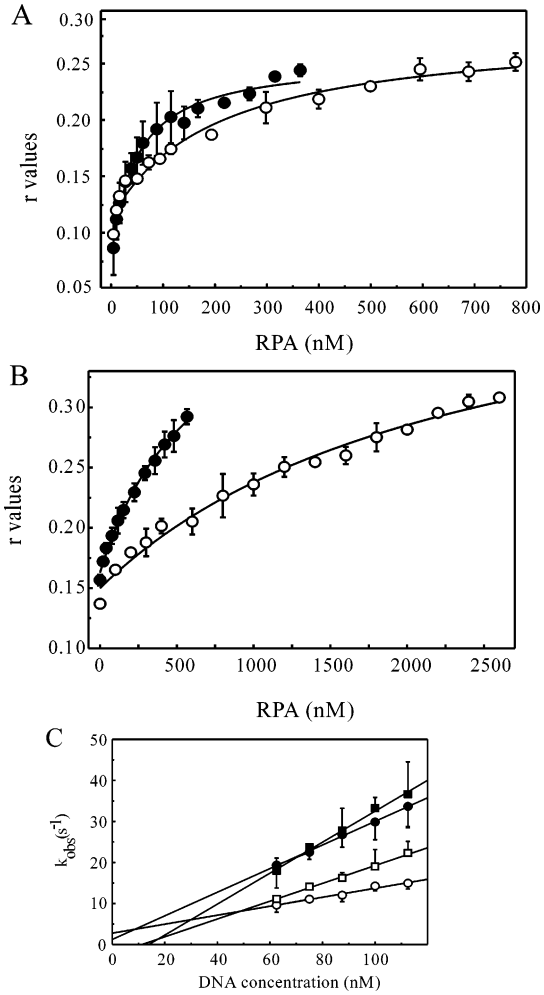

FIGURE 4: Anisotropy and stopped-flow of RPA binding duplex DNA. DNA binding analysis of phosphorylated RPA on duplex DNA substrates. (A) Fluorescence polarization analysis of RPA (filled circles) and hyperphosphorylated RPA (open circles) binding to a duplex DNA containing a cisplatin 1,2 d(GpG) adduct. (B) Fluorescence polarization analysis of RPA (filled circles) and hyperphosphorylated RPA (open circles) binding undamaged duplex DNA. (C) Stopped-flow kinetic analysis of rhRPA and hyperphosphorylated RPA binding duplex 1,2d(GpG) and 1,3d(GpXpG) cisplatin damaged 30-mer DNA. The kinetic traces from 10 to 12 measurements were fit to a double exponential decay, and the observed rate constants for the fast phase of the reaction were plotted versus DNA concentration (62.5−112.5 nM). The plots of the 1,2d(GpG) (circles) and 1,3d(GpXpG) (squares) cisplatin-damaged DNA for rhRPA (filled symbols) and hyperphosphorylated RPA (open symbols) were fit to a straight line. Each point on the graph represents the average of three to four individual experiments, and the error bars represent the standard deviation.

DNA even under these reaction conditions (Figure 3B). The hyperphosphorylated RPA had a dramatically reduced level of duplex DNA binding compared with rhRPA but maintains preferential binding to cisplatin-damaged DNA (Figure 3B, open squares compared with open circles). In addition, the affinity of both RPA preparations for the duplex DNA closely correlated with the denaturation activity of RPA (data not shown). These results demonstrate that RPA hyperphosphorylation inhibits duplex DNA binding, while maintaining damage-specific binding of RPA.

Fluorescence polarization binding assays were performed with duplex DNA substrates, and the results are presented in Figure 4A,B. Again, a clear decrease in affinity is observed

Table 1: Equilibrium Dissociation Constants for RPA and Hyperphosphorylated RPA Binding DNA

DNA substrate	rhRPA (nM)	hyp-RPA (nM)
ss dT_{30}[a]	7.6 ± 0.8	6.2 ± 0.5
ss purine	1.66 ± 0.1	2.55 ± 0.2
duplex cisplatin 1,2 d(GpG)	52.4 ± 8	201.4 ± 45.8
duplex undamaged	648 ± 123	2360 ± 570

[a] Reactions were performed in 1 M NaCl. All other reactions were conducted in buffer with 50 mM NaCl.

for hyperphosphorylated RPA binding either an undamaged duplex DNA or a DNA substrate containing a single, centrally located 1,2 d(GpG) cisplatin adduct. In both cases, the relative difference in affinity was decreased by approximately a factor of 4 when comparing the affinity of the hyperphosphorylated RPA for the substrate to unphosphorylated RPA (Table 1).

The effect of phosphorylation on the k_{on} of RPA for duplex DNA was then assessed to aid in our mechanistic understanding of the effect of RPA phosphorylation on duplex DNA binding (Figure 4C). Reactions were performed with duplex undamaged (data not shown), cisplatin 1,2d(GpG) (circles), and cisplatin 1,3d(GpXpG) (squares) damaged 30 bp DNA substrates. Binding reactions were initiated with rhRPA (filled symbols) or hyperphosphorylated RPA (open symbols), and fluorescence traces were obtained. Analyses of these data revealed that the k_{on} of rhRPA for the 1,3d-(GpXpG) was 0.377 ± 0.06 nM^{-1} s^{-1} and 0.288 ± 0.04 nM^{-1} s^{-1} for the DNA substrate containing the 1,2d(GpG) DNA cisplatin adduct. These data are consistent with the observation that RPA has higher affinity for duplex DNA substrates with a greater degree of distortion and unwinding of the duplex DNA structure. The k_{on} of hyperphosphorylated RPA was determined to be 0.217 ± 0.028 and 0.109 ± 0.018 nM^{-1} s^{-1} for the 1,3d(GpXpG) and 1,2d(GpG) DNA substrates, respectively. The k_{on} of rhRPA for the undamaged duplex DNA was determined to be 0.047 ± 0.006 nM^{-1} s^{-1}, while we were unable to determine the k_{on} of hyperphosphorylated RPA due to the lack of sufficient DNA binding (data not shown). These data demonstrate that the k_{on} ratio between rhRPA and hyperphosphorylated RPA for the 1,3d-(GpXpG) is 1.74 compared with 2.64 for the 1,2d(GpG) cisplatin DNA substrate. This indicates that the greater the duplex structural distortion in the DNA the less difference in duplex DNA binding is observed between RPA and hyperphosphorylated RPA. This interpretation is also consistent with the ssDNA binding analysis in which a greater difference in binding between unphosphorylated and hyperphosphorylated RPA is observed when measuring binding to lower affinity DNA substrates.

Effect of RPA Phosphorylation on DNA Repair. RPA plays a critical role in NER and is thought to be involved in the rate-limiting step of NER, the damage recognition process. While we have observed effects of hyperphosphorylation of RPA on duplex DNA binding, a previous report convincingly demonstrated that a phosphorylated form of RPA was fully functional in the in vitro NER assay (*18*). To assess whether our hyperphosphorylated form of RPA was capable of functioning in NER, we performed in vitro DNA incision assays using HeLa cell-free extracts in which RPA was immunodepleted. The DNA substrate was an internally

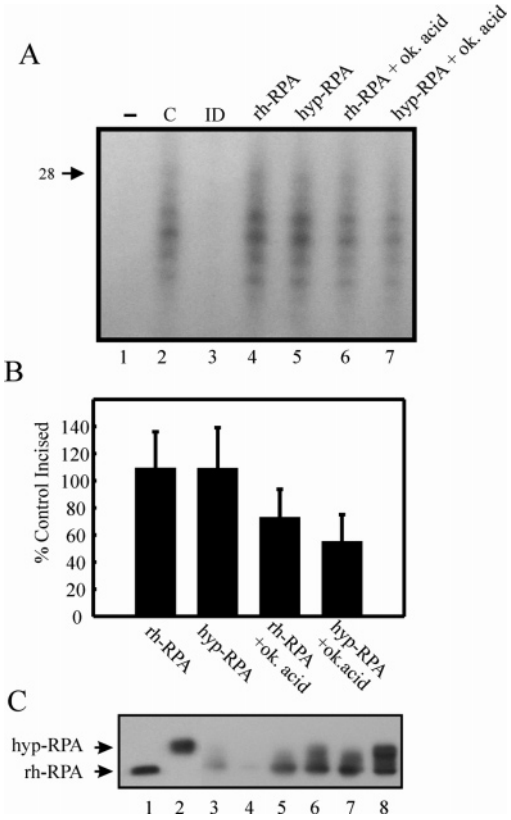

FIGURE 5: In vitro DNA repair assay using rhRPA and hyperphosphorylated RPA. HeLa crude extracts were added to a 120 bp DNA containing a cisplatin 1,3d(GpXpG) DNA adduct. Incision of the DNA substrate was visualized on 8% polyacrylamide−7 M urea sequencing gels. (A) Lane 1 is the control with no added extract, and lane 2 (C) is the control with the addition of crude extract; lane 3 (ID) is the RPA immunodepleted extracts; lanes 4 and 5 are immunodepleted extracts with the addition of 300 ng of rhRPA or hyperphosphorylated RPA, respectively; lanes 6 and 7 are immunodepleted extracts with the addition of 0.1 μM okadaic acid for rhRPA and hyperphosphorylated RPA, respectively. (B) Quantification of incision using the control value (crude extract containing endogenous RPA) as 100% incised. (C) Western blot analysis of the incision reactions. Lanes 1 and 2 are input controls for rhRPA and hyperphosphorylated RPA prior to the incision reaction, respectively; lane 3 is the endogenous RPA present in the crude extract; lane 4 is the RPA immunodepleted extracts; lanes 5 and 6 are the rhRPA and hyperphosphorylated RPA following the incision reaction, respectively; lanes 7 and 8 are the rhRPA and hyperphosphorylated RPA following the incision reaction in the presence of okadaic acid, respectively.

labeled 120 bp DNA containing a centrally positioned 1,3d-(GpXpG) DNA adduct. The control lanes for the incision experiment include the DNA substrate only and HeLa crude extracts with endogenous RPA (Figure 5A, lanes 1 and 2, respectively). An undamaged DNA substrate was also used as a control and resulted in no incision (data not shown). HeLa extracts, immunodepleted to remove the endogenous RPA, had minimal incision of the DNA substrate (Figure 5A, lane 3). Both RPA and hyperphosphorylated RPA were capable of restoring NER activity (Figure 5A, lanes 4 and 5, respectively). The addition of okadaic acid to the reactions resulted in a decreased level of incision (Figure 5A, lanes 6 and 7), consistent with previous results (*19*). The quantification of the results revealed a minimal difference in incision between extracts supplemented with rhRPA and hyperphosphorylated RPA (Figure 5B). The crude extract with endogenous RPA was used as the control and estab-

lished the 100% incision value. The increase observed above 100% for both rhRPA and hyperphosphorylated RPA is most likely the result of addition of RPA above the endogenous level of protein in the control extracts (as seen in the Western blot analysis in Figure 5C). The presence of the okadaic acid helps maintain the hyperphosphorylation of RPA as seen in Western blot analysis performed after the incision reactions (Figure 5C). Titration of RPA and time course experiments also demonstrated minimal difference in the incision with rhRPA and hyperphosphorylated RPA (data not shown). These data demonstrate that RPA hyperphosphorylation has minimal effect on DNA incision in an in vitro DNA repair system, consistent with previous data.

RPA Hyperphosphorylation Alters in Vitro DNA Replication. RPA is required for SV40 in vitro DNA replication. To assess whether RPA hyperphosphorylation affects DNA replication, we performed in vitro DNA replication assays using the SV40 system and hypotonic HeLa cell extracts that were immunodepleted of RPA (Figure 6A, lanes 1 and 4). Typically, large T-antigen is the last agent added, which serves to initiate the replication reaction. However, we observed that within this short time the hyperphosphorylated RPA was converted to a predominantly dephosphorylated form (Figure 6A, lane 3). We found that by adding RPA last to the reaction we were able to preserve the phosphorylated form in the replication reaction (Figure 6A, lane 6).

Analysis of the DNA replication products was performed by agarose gel electrophoresis (Figure 6B). The control lanes for the replication experiment include the extracts containing endogenous RPA without T-Ag (lanes 1 and 6) or with the addition of large T-antigen (lanes 2 and 7). The replication extracts were immunodepleted to remove the endogenous RPA, which resulted in minimal nucleotide incorporation (Figure 6B, lane 3 and 8, respectively). Either rhRPA or hyperphosphorylated RPA was added to the reactions. If hyperphosphorylated RPA was added before large T-antigen and allowed to become dephosphorylated, there was very little difference in replication activity between rhRPA and hyperphosphorylated RPA-supplemented extracts (lanes 4 and 5). When RPA was added as the final component to the reactions, a difference in replication products was observed (lanes 9 and 10). The increase in DNA replication activity with the addition of either RPA compared with the control (nondepleted extract) is likely the result of an increase in the amount of RPA in the replication reaction (data not shown). Quantification of the amount of Form I DNA reveals an approximate 50% decrease in replication activity between rhRPA and hyperphosphorylated RPA-supplemented extracts (Figure 5C). In addition, time course and titration experiments were also performed with similar results (data not shown). These data demonstrate that RPA hyperphosphorylation results in a decrease in replication activity in an in vitro DNA replication system.

RPA Hyperphosphorylation Affects Protein−Protein Interactions in Vitro. Our results demonstrate that RPA hyperphosphorylation has no effect on DNA incision in an in vitro DNA repair system. This would suggest that hyperphosphorylation of RPA would have a minimal effect on RPA protein−protein interaction with NER proteins. However, the decrease observed in in vitro replication activity would suggest that there may be a difference in RPA protein−protein interactions with replication proteins. To

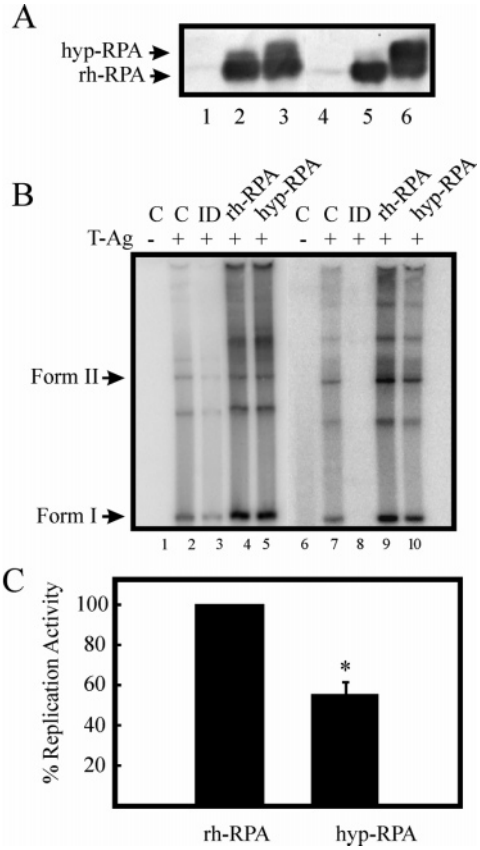

FIGURE 6: In vitro DNA replication assay using rhRPA and hyperphosphorylated RPA. (A) Western blot analysis of RPA-p34 in the replication reactions. In vitro DNA replication reactions were prepared using RPA-immunodepleted extract as described in Materials and Methods. The extracts were supplemented with buffer (lanes 1 and 4), rhRPA (lanes 2 and 5), or hyperphosphorylated RPA (lanes 3 and 6). In lanes 2 and 3, the RPA was added prior to T-antigen, while in lanes 5 and 6 the RPA was added as the last component to the reaction mix. Reactions were incubated for 2 h, and then proteins were separated by SDS−PAGE and RPA p34 phosphorylation status was measured by Western blot. (B) Analysis of DNA replication products by agarose gel electrophoresis. Lane 1 is the control without T-antigen added, and lane 2 is the complete reaction including T-antigen; lane 3 is from a reaction performed with the extract immunodepleted of RPA; lanes 4 and 5 are immunodepleted extracts with 150 ng of rhRPA or hyperphosphorylated RPA added prior to T-antigen. Lanes 6−10 are from identical reactions except the RPA was added as the last component to the reactions. (C) Quantification of the pZ189 replication generating Form I DNA. PhosphorImager analysis of the gel was performed quantifying Form I DNA, and the activity obtained with the immunodepleted extract supplemented with rhRPA was set to represent 100% replication.

address this question, we performed co-immunoprecipitation analyses comparing RPA and hyperphosphorylated RPA with respect to interaction with the XPA protein and DNA pol α, respectively. Each purified protein (see Methods) was incubated with RPA and then precipitated with its own specific antibody, and both the supernatant (S) and the immunoprecipitate (P) were analyzed by Western blot analysis using the RPA-p34 antibody. The hyperphosphorylated RPA and rhRPA both associate equally well with the XPA protein (Figure 7A, top panel lanes 1−4). These results demonstrate that RPA phosphorylation does not affect the interaction between RPA and XPA. The DNA pol α protein associates strongly with rhRPA, and this association is disrupted by phosphorylation (Figure 7A, bottom panel,

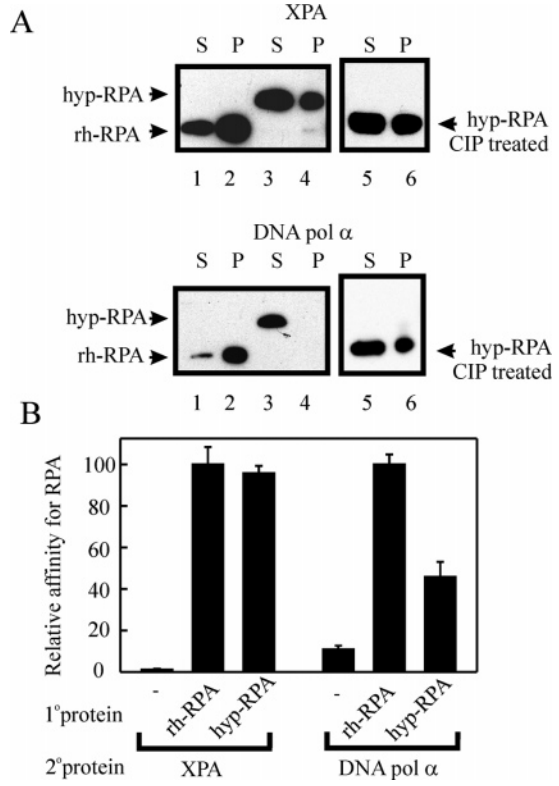

FIGURE 7: Hyperphosphorylation of RPA differentially alters protein−protein interactions. (A) Co-immunoprecipitation of RPA with either XPA or DNA pol α Purified rhRPA (lanes 1 and 2), hyperphosphorylated RPA (lanes 3 and 4), and hyperphosphorylated RPA that was treated with CIP (lanes 5 and 6) was mixed with purified XPA or DNA pol α for 30 min on ice. The mixture was incubated further with anti-XPA or anti-DNA pol α overnight at 4 °C. The proteins that were immunoprecipitated with protein G-agarose (P) or remained in the supernatant (S) were separated by SDS−PAGE and RPA-p34 was detected by Western blotting. The arrowheads indicate the position of the RPA-p34 subunit. (B) Protein−protein interaction between RPA and DNA pol α or XPA detected with an ELISA assay. A modified ELISA was performed as described under Materials and Methods. Wells were coated with 100 ng of either rhRPA or hyperphosphorylated RPA. The wells were then blocked and 0.5×, 1×, or 2× molar ratio of the secondary protein was added and incubated. Primary antibody directed against either XPA or DNA pol α was added followed by the addition of the HRP-conjugated secondary antibody. The absorbance at 652 nm was measured over a period of 15 min. The results are presented as "Relative affinity for RPA" with the value obtained for rhRPA representing 100%.

lanes 1−4) consistent with the decrease in replication activity observed with RPA phosphorylation. Different concentrations of RPA in the immunoprecipitation analysis resulted in similar results (data not shown).

To determine if the RPA phosphorylation effect on RPA protein−protein interactions with DNA pol α was reversible, calf intestinal phosphatase (CIP) was used to dephosphorylate hyperphosphorylated RPA, and the immunoprecipitation experiments were repeated (Figure 7A, lanes 5 and 6). Treatment of hyperphosphorylated RPA with CIP resulted in a form of RPA that migrated similar to the rhRPA protein as determined by single dimension SDS−PAGE. The CIP-treated hyperphosphorylated RPA interacts with XPA to the same extent as untreated hyperphosphorylated RPA, as expected, since no difference in the ability to interact with XPA was observed between the rhRPA and hyperphosphorylated RPA (Figure 7A, top panel, lanes 5 and 6). CIP treatment of hyperphosphorylated RPA resulted in an increased interaction with DNA pol α compared with untreated hyperphosphorylated RPA (Figure 7A, bottom panel, compare lanes 4 and 6). The minimal interaction of hyperphosphorylated RPA and DNA pol α and the restoration of interaction upon dephosphorylation of RPA strongly suggest that phosphorylation can play a major role in RPA−protein interactions and may regulate the biological functions of RPA.

We utilized an ELISA assay to quantify the protein−protein interactions that were observed in the presence and absence of RPA phosphorylation. ELISA plates, coated with either rhRPA or hyperphosphorylated RPA, were incubated with either XPA or DNA pol α, and then bound protein was detected with anti-XPA or anti-DNA pol α. Essentially, no protein binding activity was detected in the absence of RPA (Figure 7B). No difference was observed between RPA and hyperphosphorylated RPA interaction with XPA, whereas a 60% decrease was observed in hyperphosphorylated RPA interaction with DNA pol α as compared to RPA (Figure 7B), confirming the observations from the co-immunoprecipitation assays. These data suggest RPA phosphorylation may inhibit DNA replication by disrupting or inhibiting the interaction between RPA and DNA pol α, while having a minimal effect on NER as suggested by the unaltered interaction with the XPA protein.

DISCUSSION

The posttranslational phosphorylation of RPA during the normal cell cycle and in response to DNA damage is well established (*20*, *34*, *35*). How these modifications alter the role of RPA in the many DNA metabolic pathways in which it participates remains largely unknown. Recently, we have demonstrated that an intermediately phosphorylated form of RPA specific to the mitotic phase of the cell cycle displayed a decrease in duplex DNA binding/destabilization activity but displayed no difference in binding to pyrimidine-rich ssDNA (*11*). In support of this finding, a subsequent study utilized a mutant form of RPA in which eight serine residues were replaced by aspartic acid to mimic N-terminal phosphorylation of the p34 subunit of RPA (RPA32Asp8) (*17*); this RPA mutant also displayed a decrease in duplex DNA destabilization activity (*17*). In the present report, we have characterized a purified hyperphosphorylated form of RPA that resembles the damage-specific hyperphosphorylated form of RPA (*36*). Our results demonstrate that this purified, phosphorylated form of RPA displays a significant decrease in the ability to bind/destabilize duplex DNA compared to the unphosphorylated form of RPA. Damage-specific DNA binding was maintained by the hyperphosphorylated form of RPA, although its overall duplex DNA binding activity was significantly reduced compared to the unphosphorylated RPA. While no difference in affinity for pyrimidine-rich ssDNA was observed, we did observe that the phosphorylated form of RPA displayed a slight decrease in the ability to bind purine-rich ssDNA, and these data suggest a structural change in RPA that occurs upon phosphorylation that ultimately affects RPA binding to DNA substrates and decreases DNA binding affinity. This also implies that the different OB (oligonucleotide/oligosaccharide) DNA binding domains within RPA play different roles in binding to various

DNA substrates and RPA phosphorylation status affects these domains uniquely.

In NER, RPA plays a critical role in DNA damage recognition and acts as a nucleation point to direct the endonucleases XPF-ERCC1 and XPG to the damaged DNA strand (*37*−*39*). The DNA damage-dependent hyperphosphorylation of RPA has been reported to have no effect on the ability of RPA to function in NER (*18*). Consistent with these data, we observed a minimal difference in NER activity with purified hyperphosphorylated RPA in a similar in vitro incision DNA repair assay. Despite the findings that phosphorylated RPA is competent for NER, the function of phosphorylation of RPA may involve decreasing duplex DNA destabilization activity of RPA, a function also attributed to XPA, to maintain a defined nucleation point around the DNA lesion (*30*). The destabilization activity of RPA most likely plays a greater role in DNA replication in which melting small regions of secondary DNA structure is a prerequisite for DNA polymerases. Another possibility is that the duplex DNA binding/destabilization activity plays a minimal role in NER, which is consistent with a previous report (*40*).

To investigate the functional role of RPA hyperphosphorylation in DNA replication we employed the well-established in vitro SV40 DNA replication system (*31*, *41*, *42*). Our results with this system reveal a 50% decrease in SV40 DNA replication activity with hyperphosphorylated RPA. This differs from a report in the literature in which both unphosphorylated RPA and a mixture of multiple phosphorylated forms of RPA were found to be equally active in supporting SV40 DNA replication (*18*). However, the RPA preparation used in the previous report contains a large proportion of what appears to be the cell cycle-dependent isoform of RPA that is normally present throughout S-phase, and this form may stimulate DNA replication in the extract (*18*). The highly purified hyperphosphorylated RPA used here is similar to the hyperphosphorylated form that is induced in response to DNA damage. Thus, the disparity between these results may be due to functional differences between different phospho-isoforms or perhaps differences in assay conditions. The presence of the hyperphosphorylated form of RPA has also been correlated with reduced DNA replication activity in extracts from UV-irradiated and adozelesin-treated cells (*16*, *20*, *21*). The loss of replication activity was restored by the addition of unphosphorylated RPA (*20*). While the restoration of replication activity by the addition of unphosphorylated RPA suggested that hyperphosphorylation of RPA may be one of the mechanisms regulating DNA replication activity, these studies did not directly address the effect of hyperphosphorylated RPA on DNA replication activity. Here we demonstrate, by developing a method to produce and purify only the hyperphosphorylated form of RPA, direct evidence that hyperphosphorylation of RPA decreases SV40 DNA replication activity. Interestingly, the loss of DNA replication activity correlates with the decrease in protein interaction observed with DNA pol α. RPA is known to stimulate both the primase activity and the processivity of DNA polymerase α (*1*). The RPA-p70 subunit interacts with the primase subunits of the polymerase (*43*). One of the interaction sites is located within residues 1−170 of the RPA-70 subunit. Recent studies with NMR demonstrated a direct interaction between an aspartic acid-substituted RPA-p34 mutant peptide (a phosphorylation mimic) and the first 170 residues of the RPA-p70 subunit, while the unphosphorylated RPA-p34 peptide did not interact (*44*). This phosphorylation-dependent conformational change in RPA may explain the decreased RPA−DNA polymerase α interactions observed here with hyperphosphorylated RPA. The loss of replication activity also correlates with a decrease in duplex DNA binding. Duplex DNA binding is directly proportional to RPA's ability to denature DNA, suggesting that hyperphosphorylation of RPA decreases duplex DNA denaturation activity (*24*). Recently, Binz et al. demonstrated a decrease in denaturation of duplex DNA using an aspartic acid-substituted RPA-p34 mutant (*17*). These data support a model by which hyperphosphorylation of RPA modulates the initiation and elongation steps of DNA replication through its effect on RPA denaturation activity and interaction with DNA polymerase α.

Our results are consistent with the hypothesis that DNA damage induced hyperphosphorylation of RPA acts as a molecular switch to turn off DNA replication while maintaining DNA repair activity.

ACKNOWLEDGMENT

We acknowledge Katherine Pawelczak for critical reading of the manuscript.

REFERENCES

1. Wold, M. S. (1997) Replication protein A: a heterotrimeric, single-stranded DNA-binding protein required for eukaryotic DNA metabolism. *Annu. Rev. Biochem. 66*, 61−92.
2. Iftode, C., Daniely, Y., and Borowiec, J. (1999) Replication protein A (RPA): the eukaryotic SSB, *Crit. Rev. Biochem. Mol. Biol. 34*, 141−180.
3. Brosh, R. M., Orren, D. K., Nehlin, J. O., Ravn, P. H., Kenny, M. K., Machwe, A., and Bohr, V. A. (1999) Functional and physical interaction between WRN helicase and human replication protein A, *J. Biol. Chem. 274*, 18341−18350.
4. He, Z., Henricksen, L. A., Wold, M. S., and Ingles, C. J. (1995) RPA involvement in the damage-recognition and incision steps of nucleotide excision repair, *Nature 374*, 566−569.
5. Bohr, V. A., Cooper, M., Orren, D., Machwe, A., Piotrowski, J., Sommers, J., Karmakar, P., and Brosh, R. (2000) Werner syndrome protein: biochemical properties and functional interactions, *Exp. Gerontol. 35*, 695−702.
6. Wakasugi, M., Shimizu, M., Morioka, H., Linn, S., Nikaido, O., and Matsunaga, T. (2001) Damaged DNA-binding protein DDB stimulates the excision of cyclobutane pyrimidine dimers in vitro in concert with XPA and replication protein A, *J. Biol. Chem. 276*, 15434−15440.
7. Matsuda, T., Saijo, M., Kuraoka, I., Kobayashi, T., Nakatsu, Y., Nagai, A., Enjoji, T., Masutani, C., Sugasawa, K., and Hanaoka, F. (1995) DNA repair protein XPA binds replication protein A (RPA), *J. Biol. Chem. 270*, 4152−4157.
8. Braun, K., Lao, Y., He, Z., Ingles, C., and Wold, M. (1997) Role of protein−protein interactions in the function of replication protein A (RPA): RPA modulates the activity of DNA polymerase alpha by multiple mechanisms, *Biochemistry 36*, 8443−8454.
9. de Laat, W. L., Appeldoorn, E., Sugasawa, K., Weterings, E., Jaspers, N. G., and Hoeijmakers, J. H. (1998) DNA-binding polarity of human replication protein A positions nucleases in nucleotide excision repair, *Genes Dev. 12*, 2598−2609.
10. Golub, E., Gupta, R., Haaf, T., Wold, M., and Radding, C. (1998) Interaction of human rad51 recombination protein with single-stranded DNA binding protein, RPA, *Nucleic Acids Res. 26*, 5388−5393.
11. Oakley, G. G., Patrick, S. M., Yao, J. Q., Carty, M. P., Turchi, J. J., and Dixon, K. (2003) RPA phosphorylation in mitosis alters DNA binding and protein- protein interactions, *Biochemistry 42*, 3255−3264.

12. Dutta, A., and Stillman, B. (1992) cdc2 family kinases phosphorylate a human cell DNA replication factor, RPA, and activate DNA replication, *EMBO J. 11*, 2189−2199.
13. Shao, R. G., Cao, C. X., Zhang, H. L., Kohn, K. W., Wold, M. S., and Pommier, Y. (1999) Replication-mediated DNA damage by camptothecin induces phosphorylation of RPA by DNA-dependent protein kinase and dissociates RPA: DNA-PK complexes, *EMBO J. 18*, 1397−1406.
14. Brush, G. S., Anderson, C. W., and Kelly, T. J. (1994) The DNA-activated protein kinase is required for the phosphorylation of replication protein A during simian virus 40 DNA replication, *Proc. Natl. Acad. Sci., U.S.A. 91*, 12520−12524.
15. Abramova, N. A., Russell, J., Botchan, M., and Li, R. (1997) Interaction between replication protein A and p53 is disrupted after UV damage in a DNA repair-dependent manner, *Proc. Natl. Acad. Sci., U.S.A. 94*, 7186−7191.
16. Park, J. S., Park, S. J., Peng, X. D., Wang, M., Yu, M. A., and Lee, S. H. (1999) Involvement of DNA-dependent protein kinase in UV-induced replication arrest, *J. Biol. Chem. 274*, 32520−32527.
17. Binz, S. K., Lao, Y., Lowry, D. F., and Wold, M. S. (2003) The phosphorylation domain of the 32-kDa subunit of replication protein a (RPA) modulates RPA-DNA interactions − Evidence for an intersubunit interaction, *J. Biol. Chem. 278*, 35584−35591.
18. Pan, Z. Q., Park, C. H., Amin, A. A., Hurwitz, J., and Sancar, A. (1995) Phosphorylated and unphosphorylated forms of human single-stranded DNA-binding protein are equally active in simian virus 40 DNA replication and in nucleotide excision repair, *Proc. Natl. Acad. Sci., U.S.A. 92*, 4636−4640.
19. Ariza, R. R., Keyse, S. M., Moggs, J. G., and Wood, R. D. (1996) Reversible protein phosphorylation modulates nucleotide excision repair of damaged DNA by human cell extracts, *Nucleic Acids Res. 24*, 433−440.
20. Carty, M. P., Zernik-Kobak, M., McGrath, S., and Dixon, K. (1994) UV light-induced DNA synthesis arrest in HeLa cells is associated with changes in phosphorylation of human single-stranded DNA-binding protein, *EMBO J. 13*, 2114−2123.
21. Liu, J. S., Kuo, S. R., McHugh, M. M., Beerman, T. A., and Melendy, T. (2000) Adozelesin triggers DNA damage response pathways and arrests SV40 DNA replication through replication protein A inactivation, *J. Biol. Chem. 275*, 1391−1397.
22. Liu, J. S., Kuo, S. R., Yin, X., Beerman, T. A., and Melendy, T. (2001) DNA damage by the enediyne C-1027 results in the inhibition of DNA replication by loss of replication protein a function and activation of DNA-dependent protein kinase, *Biochemistry 40*, 14661−14668.
23. Nuss, J. E., Patrick, S. M., Oakley, G. G., Alter, G. M., Robison, J. G., Dixon, K., and Turchi, J. J. (2005) DNA Damage induced hyperphosphorylation of replication protein A. 1. Identification of novel sites of phosphorylation in response to DNA damage, *Biochemistry 44*, 8438−8448.
24. Patrick, S. M., and Turchi, J. J. (1999) Replication protein A (RPA) binding to duplex cisplatin-damaged DNA is mediated through the generation of single-stranded DNA, *J. Biol. Chem. 274*, 14972−14978.
25. Patrick, S. M., and Turchi, J. J. (1998) Human replication protein A preferentially binds duplex DNA damaged with cisplatin, *Biochemistry 37*, 8808−8815.
26. Patrick, S. M., and Turchi, J. J. (2001) Stopped-flow kinetic analysis of replication protein A-binding DNA − Damage recognition and affinity for single-stranded DNA reveal differential contributions of k(on) and k(off) rate constants, *J. Biol. Chem. 276*, 22630−22637.
27. Andrews, B. J., and Turchi, J. J. (2004) Development of a high-throughput screen for inhibitors of replication protein A and its role in nucleotide excision repair, *Mol. Cancer Ther. 3*, 385−391.
28. Hermanson, I. L., and Turchi, J. J. (2000) Overexpression and purification of human XPA using a Baculovirus expression system, *Protein Exp. Purif. 19*, 1−11.
29. Reveal, P. M., Henkels, K. M., and Turchi, J. J. (1997) Synthesis of the mammalian telomere lagging strand in vitro, *J. Biol. Chem. 272*, 11678−11681.
30. Patrick, S. M., and Turchi, J. J. (2002) Xeroderma pigmentosum complementation group A protein (XPA) modulates RPA-DNA interactions via enhanced complex stability and inhibition of strand separation activity, *J. Biol. Chem. 277*, 16096−16101.
31. Li, J. J., and Kelly, T. J. (1984) Simian virus-40DNA-replication in vitro, *Proc. Natl. Acad. Sci., U.S.A. 81*, 6973−6977.
32. Carty, M. P., Hauser, J., Levine, A. S., and Dixon, K. (1993) Replication and mutagenesis of UV-damaged DNA templates in human and monkey cell-extracts, *Mol. Cell. Biol. 13*, 533−542.
33. Seidman, M. M., Dixon, K., Razzaque, A., Zagursky, R. J., and Berman, M. L. (1985) A shuttle vector plasmid for studying carcinogen-induced point mutations in mammalian-cells, *Gene 38*, 233−237.
34. Fotedar, R., and Roberts, J. M. (1992) Cell cycle regulated phosphorylation of RPA-32 occurs within the replication initiation complex, *EMBO J. 11*, 2177−2187.
35. Liu, V. F., and Weaver, D. T. (1993) The ionizing radiation-induced replication protein A phosphorylation response differs between ataxia telangiectasia and normal human cells, *Mol. Cell Biol. 13*, 7222−7231.
36. Oakley, G. G., Loberg, L. I., Yao, J. Q., Risinger, M. A., Yunker, R. L., Zernik-Kobak, M., Khanna, K. K., Lavin, M. F., Carty, M. P., and Dixon, K. (2001) UV-induced hyperphosphorylation of replication protein a depends on DNA replication and expression of ATM protein, *Mol. Biol. Cell 12*, 1199−1213.
37. de Laat, W. L., Appeldoorn, E., Sugasawa, K., Weterings, E., Jaspers, N. G. J., and Hoeijmakers, J. H. J. (1998) DNA-binding polarity of human replication protein A positions nucleases in nucleotide excision repair, *Genes Dev. 12*, 2598−2609.
38. Mu, D., Park, C. H., Matsunaga, T., Hsu, D. S., Reardon, J. T., and Sancar, A. (1995) Reconstitution of human DNA repair excision nuclease in a highly defined system, *J. Biol. Chem. 270*, 2415−2418.
39. Sugasawa, K., Ng, J. M., Masutani, C., Iwai, S., van der Spek, P. J., Eker, A. P., Hanaoka, F., Bootsma, D., and Hoeijmakers, J. H. (1998) Xeroderma pigmentosum group C protein complex is the initiator of global genome nucleotide excision repair, *Mol. Cell 2*, 223−232.
40. Riedl, T., Hanaoka, F., and Egly, J. M. (2003) The comings and goings of nucleotide excision repair factors on damaged DNA, *EMBO J. 22*, 5293−5303.
41. Melendy, T., and Stillman, B. (1991) Purification of DNA polymerase-delta as an essential simian virus-40 DNA-replication factor, *J. Biol. Chem. 266*, 1942−1949.
42. Wobbe, C. R., Dean, F. B., Murakami, Y., Weissbach, L., and Hurwitz, J. (1986) Simian virus 40 DNA replication in vitro: study of events preceding elongation of chains, *Proc. Natl. Acad. Sci., U.S.A. 83*, 4612−4616.
43. Dornreiter, I., Erdile, L. F., Gilbert, I. U., Vonwinkler, D., Kelly, T. J., and Fanning, E. (1992) Interaction of DNA polymerase-alpha primase with cellular replication protein-A and SV40-T antigen, *EMBO J. 11*, 769−776.
44. Daughdrill, G. W., Buchko, G. W., Botuyan, M. V., Arrowsmith, C., Wold, M. S., Kennedy, M. A., and Lowry, D. F. (2003) Chemical shift changes provide evidence for overlapping single-stranded DNA- and XPA-binding sites on the 70 kDa subunit of human replication protein A, *Nucleic Acids Res. 31*, 4176−4183.

BI048057B